

**THE INSTITUTE OF CHEMISTRY
OF THE ACADEMY OF SCIENCES OF MOLDOVA**

With manuscript title

UDC: 546.7:546.5:546.4(043.2)+541.13(043.2)+544.174.2(043.2)

SÎRBU DUMITRU

**SYNTHESIS, STUDY OF FERROCENE AND PORPHYRIN
DERIVATIVES AND THEIR COMPLEXES WITH TRANSITION
METALS (Fe, Co, Ni, Cu, Zn, Ru and Pd)**

141.01. INORGANIC CHEMISTRY

Summary of the doctoral thesis in chemical sciences

CHIȘINĂU – 2015

The thesis was done in the Laboratory of Bioinorganic Chemistry and Nanocomposites of the Institute of Chemistry of the Academy of Sciences of Moldova and the Molecular Photonics Laboratory of the University of Newcastle upon Tyne.

Scientific supervisor:

Turtă Constantin, Doctor Hab. in chemistry, Professor, Academician, Inorganic Chemistry

Scientific co-supervisor:

Benniston Andrew, PhD in chemistry, Professor, Photonic Energy Sciences

Official reviewers:

Arion Vladimir, Doctor Hab. in chemistry, University Professor, Inorganic Chemistry, Institute of Inorganic Chemistry – University of Vienna, Austria.

Bulimestru Ion, Doctor in chemistry, University Lecturer, Inorganic Chemistry, Moldova State University.

The membership of the Specialized Scientific Council:

1. **BULHAC Ion** – Dr. Hab. in chemistry, associate researcher – president;
2. **LAZARESCU Ana** – Dr. in chemistry, associate researcher – scientific secretary;
3. **GULEA Aurelian** – Dr. Hab. in chemistry, univ. Professor, Academician – member;
4. **VEREJAN Ana** – Dr. in chemistry, univ. lecturer – member;
5. **BÎRCĂ Maria** – Dr. in chemistry, univ. lecturer – member.

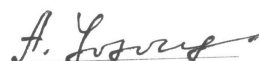
The thesis *viva* will take place on September 4, 2015 at 14:00, at the meeting of Specialized Scientific Council (D06.141.03-01) of the Institute of Chemistry of the Academy of Sciences of Moldova, Chişinău, str. Academiei, 3.

The PhD thesis and its summary may be consulted at the scientific library of the Academy of Sciences of Moldova and at N.C.A.A. Web page (www.cnaa.md).

The thesis summary has been sent on 24.07.2015.

Scientific Secretary of the Specialized Scientific Council,

Doctor in chemistry

 **Lazarescu Ana**

Scientific supervisor,

Doctor Habilitatus in chemistry, Univ. Professor, Academician

Turtă Constantin

Scientific co-supervisor,

Doctor in chemistry, Professor



Benniston Andrew

Author:



Sîrbu Dumitru

(© Sîrbu Dumitru, 2015)

CONCEPTUAL MILESTONES OF RESEARCH

Keywords: ferrocene, porphyrin, transition metal complexes, solar cell, protons reduction, UV-Vis.

The increasingly high demand of power is constantly motivating the research of new energy resources. The ecological issues generated by the greenhouse emissions have attracted much attention during the last years and either removal of the formed gases from atmosphere or the shift from fossil fuels to carbon neutral renewable energy sources are required. Solar energy is so far the largest accessible renewable energy resource, providing in one hour to the earth more energy than the humans could consume in a year. Still, for a major contribution to the global energy production, the solar energy must be harvested, converted into a useful form (chemical or electrical energy) and stored in an efficient and low cost process.

Porphyrins and comparable derivatives are ubiquitous in nature and constitute the molecular cornerstone of several light-driven processes which help maintain life on Earth. Transition metal porphyrins are well known for their applications in electrocatalysis including many industrially imperative reactions [1]. Particular attention has been paid to electrocatalytic reduction of carbon dioxide by metal (e.g., Ag, Pd, Co, Fe) porphyrin derivatives [2]. Examples of electrochemical proton reduction catalysed by metal (e.g., Co, Fe) porphyrin derivatives are also well known [3]. The good cross section capture of visible photons for the chromophores, coupled to their excellent redox excited-state behaviour are motivating the continued interest in porphyrin derivatives. Mimicry systems for artificial photosynthesis applications is certainly one major research area in which porphyrin derivatives have a special place. Coupled to fundamental studies is the application of porphyrin derivatives in areas such as sensors, photodynamic therapy sensitisers and dye sensitised solar cells (DSSC). Various light harvesting systems were constructed and studied in the past decades, including porphyrin and ferrocene containing architectures, still many challenges have to be faced in order to reach Nature photosynthetic machinery efficiency and construct economically sustainable artificial analogues.

The aim of this work was to design, synthesize and study molecules based on porphyrin and ferrocene, and to reveal structure-property relationships that would allow a better understanding of the mechanisms governing the photophysical and electrochemical processes in the designed systems. **The main objectives** aiming to achieve the purpose of this work were: the design and synthesis of molecular systems based on ferrocene and porphyrin; composition determination and structural characterization of the obtained compounds by using physico-chemical methods (IR, NMR, Atomic Absorption, Mass Spectrometries, Elemental Analysis and X-ray crystallography); study of the photophysical and electrochemical properties of the materials

by various methods (Mössbauer, UV-Vis absorption and Ultrafast Transient Absorption Pump-Probe spectrometries, cyclic voltammetry, UV-Vis spectroelectrochemistry); revealing the structure-property relationships determining physico-chemical properties by using the information obtained from previous objectives; study of the applicative potential for the examined materials.

The thesis consists of an introduction, four chapters, overall conclusions and recommendations, bibliography of 223 references and 14 annexes comprising of 24 figures. 128 pages of main text contain 90 figures, 11 tables and two equations. The thesis is devoted to a number of research topics which are followed within its sections. Following the aspiration to enrich the understanding of processes chosen and refined by the genius of Nature, this work is giving some answers and conclusions that are expected to be useful for further research both in our and any other teams working in similar or related area. In Chapter 1 a review is given on the work done by various research groups worldwide on study of molecular systems based on ferrocene and porphyrin. The achievement of thesis objectives is fully described in the Chapters 2 – 4, that comprise the experimental work done on the synthesis and thorough study of 1,1'-ferrocene disubstituted products and ferrocene-porphyrin conjugates. A new simple route for desymmetrizing ferrocene was found based on selective oxidation of only one aldehyde unit in 1,1'-ferrocenedicarboxaldehyde to give 1'-formyl-ferrocenecarboxylic acid. As it was shown by engaging the both oxidation products of 1,1'-ferrocenedicarboxaldehyde into classical organic reactions and further complexation (Fe(II), Ru(II)), the simple chromatography-free method elaborated for desymmetrizing ferrocene molecule is an alternative route to 1,1'-asymmetrical ferrocenes that could find practical applications in industrial catalytic processes [4]. The 1'-(3,5-dihydroxy-2-picolinoyl-3,5-di(pyridin-2-yl)cyclohexyl)-ferrocene-carboxylic acid is a promising candidate in the exploration of host-guest interactions in aqueous media with small molecules like aminoacids. The new, rarely isolated halfway product in the BODIPY synthesis, namely 1,1'-ferrocene-bis[2-(4-ethyl-3,5-dimethylpyrro)methanone], was found to be stable and reacted with $\text{BF}_3 \cdot \text{Et}_2\text{O}$ to produce the bis(difluoropyrrolo-oxaborole) compound, which is only the third example of ketopyrrole- BF_2 adduct described in the literature. Beside the fundamental interest, it was found that the reactivity of electrochemically generated ferrocenium ion could be used for nucleophiles redox sensing by the 2-ketopyrrole intermediate, while its bis- BF_2 complex may potentially be applied as a dark-state energy transfer quencher for fluorophores which emit between 500 and 600 nm. The ferrocene-porphyrin dye obtained within this work was employed as sensitizer for TiO_2 surface in a Grätzel solar cell and the key processes governing the system were described using cyclic voltammetry and UV-Vis transient absorption spectroscopy. The

conclusions made in this work could be helpful to guide further design of porphyrin-sensitised solar cells. A tentative mechanism of electrochemical hydrogen production, catalysed by Pd(II) and Cu(II) *meso*-tetraferrocenyl porphyrin complexes, was proposed consisting of phlorin mediated pathway and a feasible explanation of ferrocene units role was suggested. These results are giving some valuable information for the construction of alternative materials for electrocatalysis of proton reduction reaction, based on non-metal redox processes.

The thesis is based on four research papers in journals with impact factor 2.379 - 4.197 (*RSC Advances*, *European Journal of Inorganic Chemistry*, *Tetrahedron Letters*, *Dalton Transactions*) [5,6,7] and one without co-authors in journal of B grade (UIF 0.135) - *Chemistry Journal of Moldova. General, Industrial and Ecological Chemistry* [8]. Additionally, a review material related and partially used in this thesis was published in the Chapter 3 of book *Management of Water Quality in Moldova* [9]. The research results were presented in poster (seven abstracts) and one oral sessions at national and international scientific conferences, symposiums, summer schools. Some aspects of the research process were disseminated at scientific TV show: “*Știință și inovare*”, TeleRadioMoldova, 28th December 2013 and 11th of January 2014. The very quick citation of our work is encouraging our fair attempts.

The solved scientific problem consists of elucidating the structure-property relationship in the molecular systems based on ferrocene and porphyrin, contributing to a deeper understanding of the physical and chemical processes in the materials studied, for further optimization of their practical efficiency.

The main scientific results submitted for approval are:

- New pathway for desymmetrisation of ferrocene via oxidation of 1,1'-ferrocene dicarboxaldehyde was developed, offering an alternative approach to potentially useful asymmetrical products;
- 1,1'-Ferrocene bis(2-(4-ethyl-3,5-dimethylpyrro)methanone) obtained within this thesis was proved to be a useful material for redox sensing of nucleophiles, while its bis-BF₂ chelate is only the third published example of ketopyrrole-BF₂ complexes.
- For the first time a ferrocene-porphyrin dye was employed as sensitiser for TiO₂ surface in a Grätzel cell and the key processes governing the system efficiency were analysed.
- New alternative, metal tetraferrocenylporphyrin based, electrocatalysts for protons reduction to molecular hydrogen were obtained and a feasible catalysis mechanism was proposed.

THESIS CONTENT

The **Introduction** is giving information on the actuality and importance of the addressed issue within the research area, the aim and main objectives, the originality of results, fundamental and applicative aspects of results, dissemination and publication of the research findings, thesis overview and the keywords.

1. DERIVATIVES OF FERROCENE AND PORPHYRIN – A LITERATURE REVIEW ON THE STRUCTURE, PHYSICO-CHEMICAL PROPERTIES AND APPLICATIONS

In this chapter a review is given on the work done by various research groups worldwide on the synthesis, study and applications of molecular systems based on ferrocene and porphyrin, highlighting the processes associated and inspired by natural photosynthesis. A brief introduction to the porphyrins structure and general properties is followed by the summary on the main synthetic routes to construct the porphyrin molecule. The next section is giving a short analysis of the modified chlorophyll and synthetic porphyrin dyes for sensitisation of TiO₂ surface in DSSCs, aiming to illustrate the structure-property relationships determining the device efficiency. The last section is reviewing the ferrocene containing molecular systems, including ferrocene-porphyrin conjugates, focusing on the light induced processes and the role of ferrocene unit.

2. DERIVATIVES OF 1,1'-DISUBSTITUTED FERROCENE

In the first section, a new simple chromatography-free method for desymmetrizing ferrocene is described and the use of two products obtained by partial oxidation of 1,1'-dicarboxaldehyde to obtain five new asymmetrical derivatives. The second part comprises the synthesis and thorough description of ferrocene-based difluoropyrrolo-oxaborole derivative, obtained from the halfway product in the boron-dipyrrromethene synthesis. A potential application as a dark-state energy transfer quencher, or redox reporter for the non-chelated intermediate, is proposed.

2.1. New pathway to asymmetrical ferrocenes via oxidation of 1,1'-ferrocene dicarboxaldehyde [5, 8]

The oxidation of ferrocenecarboxaldehyde using aqueous KMnO₄ in acetone is well documented to produce the corresponding carboxylic acid [10]. Repeating the literature method afforded ferrocenecarboxylic acid in reasonable yield. However, we found that the same procedure applied to **II.1** in acetone or acetonitrile did not produce the corresponding dicarboxylic acid (Figure 1). The combined evidence from NMR, IR and mass spectroscopies verified the product, from reaction performed in acetonitrile, to be 1'-formyl-ferrocenecarboxylic acid **II.2**, in which one aldehyde was oxidized but the other remained untouched. Hence, under these conditions the ferrocene is desymmetrized since it contains two different functional groups. The overall yield for **II.2** is 49 % after a fast and chromatography-free work up, providing material pure enough for further synthetic reactions.

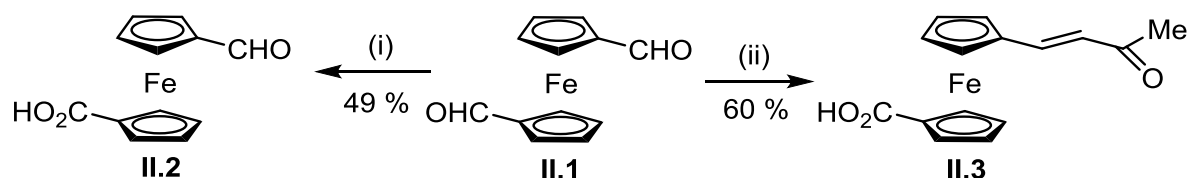


Fig. 1. Reagents and conditions: (i) KMnO_4 , $\text{CH}_3\text{CN}/\text{H}_2\text{O}$, 0°C ; (ii) KMnO_4 , acetone/ H_2O , 0°C .

A similar reaction performed using an acetone / H_2O mixture did not afford a product with NMR spectra consistent with compound **II.2**. The NMR, IR and mass spectroscopic data are fully consistent with 1'-((E)-3-oxo-but-1-enyl)-ferrocenecarboxylic acid **II.3**. We speculate that oxidation of one aldehyde to the carboxylic acid activates the other carbonyl in to condensation reaction with the acetone present in solution. Presumably for ferrocene dicarboxaldehyde the reaction of the aldehyde with acetone is too slow to compete with oxidation. Rather surprisingly, compounds **II.2** and **II.3** could not be found in the literature (SciFinder, Reaxys).

Ferrocene – terpyridine complexes

Having established the simple procedure for desymmetrizing the ferrocene, we were interested to see if useful chemical transformations could be carried out on compounds **II.2**, **II.3**. Reaction of **II.2** with 2-acetylpyridine in aqueous NaOH / NH_4OH , in a two-step one-pot Kröhnke reaction, gave after an easy column-free purification the terpy-type ligand **II.4** in 62 % yield (Figure 2).

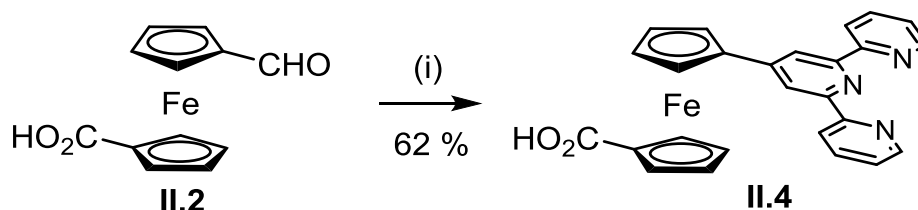


Fig. 2. Reagents and conditions: (i) 2-acetylpyridine, aq. NaOH / NH_4OH , dark.

The material is stable in the solid state, but when in a solution of methanol, DMSO or water, air-equilibrated or N_2 -purged, the compound **II.4** is extremely light-sensitive. ^1H NMR spectroscopy for **II.4** as the light-driven reaction proceeded showed that resonances for the starting material decreased and new peaks appeared with a pattern very similar to authentic $[\text{Fe}(\text{Fc-tpy})_2]^{2+}$. Both UV-vis and mass spectroscopies showed the formation of $[\text{Fe}(\text{Fc-tpy})_2]^{2+}$, hence, the source of the iron(II) must be ferrocene for the light-activated reaction to produce **FTF** $^{2+}$. It is speculated that a terpy ligand from one molecule of ground-state **II.4** bites onto the ferrocene iron(II) centre of another ‘activated’ molecule, leading to degradation of the compound. The reaction must proceed via the triplet state and the presence of the carboxylic acid unit appears to promote compound degradation. This idea was tested by reacting under the same conditions a 1:1 mixture of 1,1'-ferrocenedicarboxylic acid and terpyridine in methanol. When exposed to ambient light the solution became dark purple, with a very distinct absorption pattern suggesting

a similar degradation of the ferrocene unit and formation of the $[\text{Fe}(\text{tpy})_2]^{2+}$ complex. Non-substituted ferrocene was indefinitely stable in methanol solution in the presence of terpyridine.

Performing all steps, starting from 1,1'-ferrocenedicarboxaldehyde, under ambient light illumination gave after purification by column chromatography (silica gel, methanol) a deep purple product in 11 % yield. Suitable crystals for X-ray crystallographic analysis of the iron complex were grown, and the obtained structure confirms the identity of **FTF**(PF₆)₂ complex. The structure of the cation is illustrated in figure 3, highlighting the six-coordinate iron(II) centre and the two Fc-tpy ligands of compound **II.4**. The Fe1 – N1 (1.876 Å) and Fe1 – N4 (1.875 Å) bond lengths are typically shorter than the remaining Fe – N bond lengths (Fe1 – N2 1.974, Fe1 – N3 1.968, Fe1 – N5 1.972, Fe1 – N6 1.971 Å). A point to note is that each ferrocene group is in its carboxylic acid form and so hexafluorophosphates are present as counter-ions.

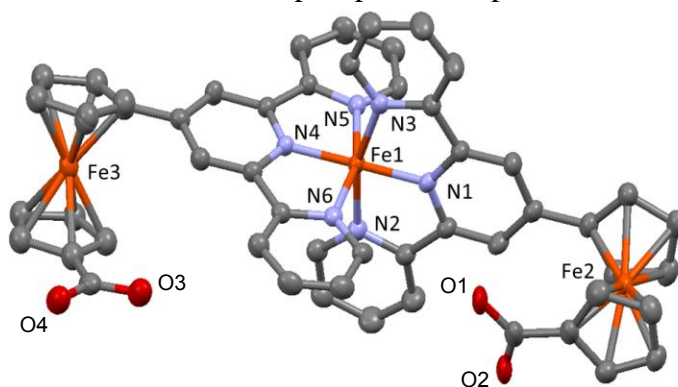


Fig. 3. X-ray diffraction molecular structure of the dication **FTF**²⁺. Counter-ions, solvent molecules, and hydrogen atoms are omitted for clarity.

Using Ru(tpy)Cl₃ as intermediate, the heteroleptic complex $[(\text{II.4})\text{Ru}(\text{tpy})]^{2+} = \text{RTF}^{2+}$ was easily obtained, as depicted in figure 4. The combined evidence from IR, NMR and accurate mass spectroscopies corroborated the structure of **RTF**(PF₆)₂.

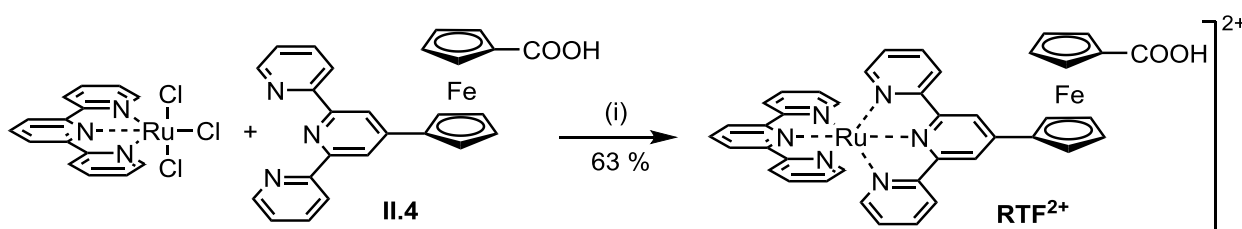


Fig. 4. Reagents and conditions: (i) N-ethylmorpholine, methanol.

A NiO based DSSC was assembled having the semiconductor surface modified with the dye **RTF**(PF₆)₂, and using solution of LiI (1.0 M) and I₂ (0.1 M) in acetonitrile as electrolyte. The short circuit current density was found to be $I_{\text{SC}} = 0.352 \text{ mA cm}^{-2}$, and the open circuit voltage $V_{\text{OC}} = -27 \text{ mV}$. The limited sensitising performance could be explained by either low absorption coefficient of the Ru(tpy)₂ derivative or poor adsorption on the NiO surface.

Michael addition products

The reaction of **II.3** with diethylmalonate in ethanol, catalysed by sodium ethoxide (Figure 5), gave after quenching with water, acidification, and purification by column chromatography (silica gel, dichloromethane / methanol 9:1) a yellow product in 35 % yield.

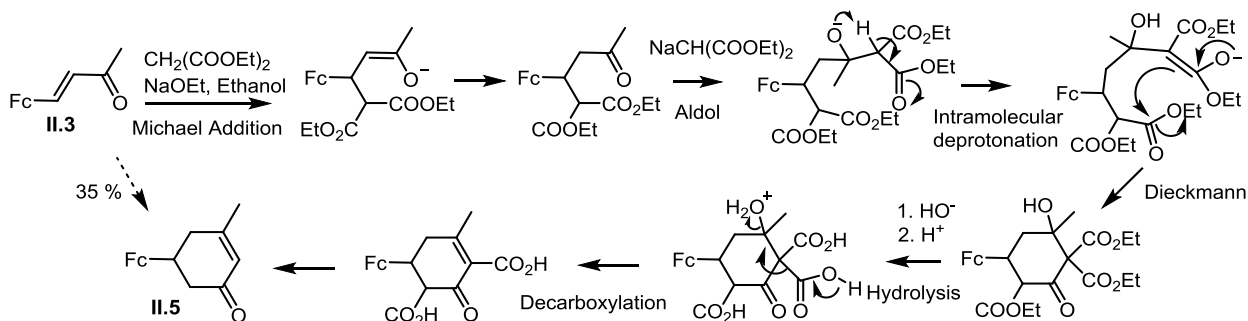


Fig. 5. Proposed mechanism to explain the formation of compound **II.5** from **II.3**. Fc = ferrocenecarboxylic acid.

The ^1H , $^{13}\text{C}\{^1\text{H}\}$, DEPT-135° and 2D homo- ($^1\text{H}/^1\text{H}$ COSY-45°), heteronuclear ($^1\text{H}/^{13}\text{C}$ HMQC and HMBC) NMR and accurate mass spectra are consistent with 1'-(5-methylcyclohex-4-en-3-one)ferrocenecarboxylic acid (**II.5**). Crystals of the compound, suitable for synchrotron X-ray analysis, were obtained. The molecular structure is shown in figure 6, and confirms unequivocally the identity of the product **II.5**. The C15 – C16 bond length of 1.354 Å is consistent with the expected double bond, and other C – C bond lengths in the cyclohexenone ring are typical for C – C single bonds. C12 is a chiral centre and both the R and S enantiomers of **II.5** are present in the crystal.

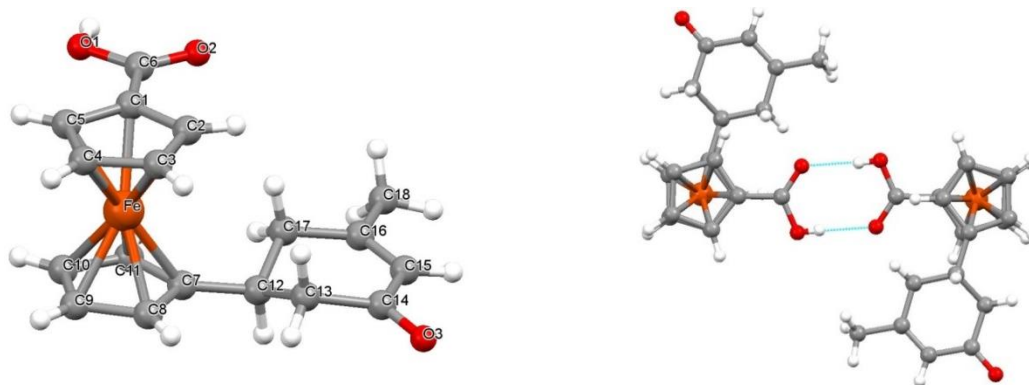


Fig. 6. X-ray diffraction molecular structure of the racemic compound **II.5** showing here the S form (left) and the centrosymmetric dimer (right).

A tentative mechanism is suggested from the initially formed Michael addition product, followed by aldol addition of the second diethyl malonate molecule and cyclohexanone ring closure through a Dieckmann condensation reaction [11]. Hydrolysis of the esters and acidification is followed by dehydration of the aldol intermediate and a series of decarboxylations to end up eventually with the identified product **II.5**. The alternative ring closure product is from a lactonization of the ketodiester intermediate.

An unexpected product was obtained in the attempt to isolate the intermediate to **II.4**. Using the identical conditions used to access **II.4**, but lacking ammonia source resulted in formation of a compound containing three pyridine rings, as suggested by elemental analysis. The NMR and ASAP/APCI-FTMS accurate mass spectra suggested a domino reaction [12] consisting of initial Claisen-Schmidt condensation and Michael addition to form the intermediate diketone, followed by double aldole reaction with the third 2-acetyl pyridine (Figure 7).

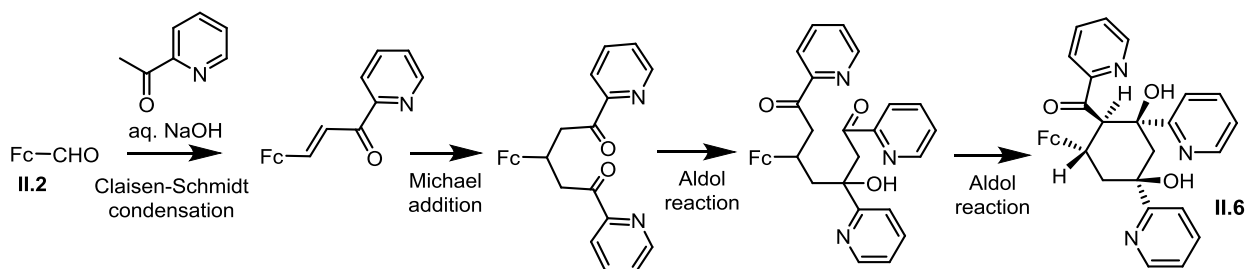


Fig. 7. The domino condensation mechanism of cyclohexyl ring formation in compound **II.6** showing the relative conformation of substituents. Fc = ferrocenecarboxylic acid.

It results in stereo- and regioselective formation of a six-membered carbocycle with four chiral centres – sodium 1'-[3,5-dihydroxy-2-picolinoyl-3,5-di(pyridin-2-yl)cyclohexyl] ferrocene carboxylate **NaII.6**, with a moderate yield 38 %. Single crystal X-ray crystallographic analysis for **II.6** showed the compound to be a racemic mixture crystallised in the triclinic space group P-1 (Figure 8). All aromatic substituents are arranged in the optimal equatorial positions, so that the four chiral atoms C12, C13, C14, C16 generate 12RS, 13SR, 14RS, 16RS configurations (S – counter clockwise rotation, R – clockwise rotation). The enantiomers of **II.5** are connected in a centrosymmetric dimer formed by typical hydrogen bonding at the carboxylic acid site (O – O distance 2.638 Å, O – H – O angle 176.2°).

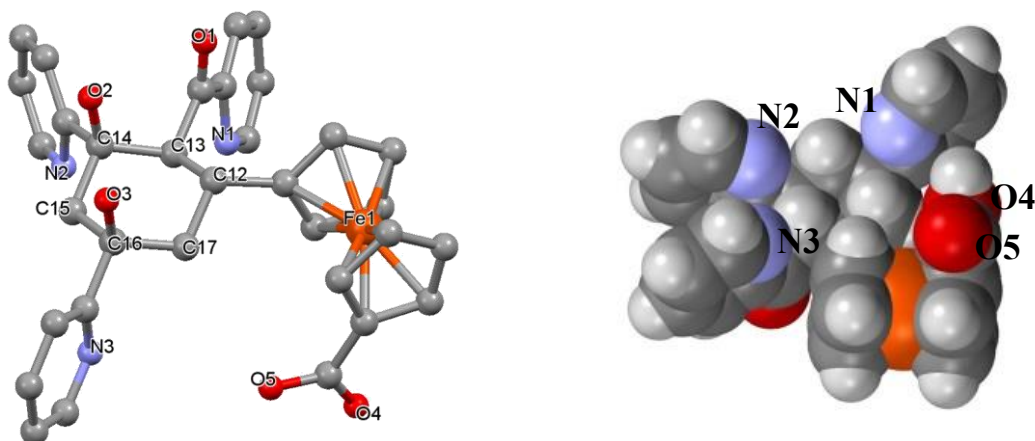


Fig. 8. The crystal structure of **II.6** showing here the RSRR form (left) and the space fill showing the internal “pocket” with N₃O₂ bonding sites (right).

The two hydroxyl groups have different arrangement for RSRR and SRSS configurations, due to four types of hydrogen bonding present in the crystal structure. An intermolecular bond of 2.904 Å (O3 – H_{O3} – O3' 170.5°) is generating a racemic dimer by connecting the two

enantiomers. The three pyridine rings and ferrocene carboxylic acid form a “pocket” (Figure 8), suitable for hosting small molecules with groups able to interact through hydrogen or ionic bonding with pyridine-N atoms and carboxylic acid-O atoms. Keeping this in mind we studied the host-guest interactions of **II.6** with a series of α -amino acids. In order to make the intermolecular interactions more pronounced, the pyridine groups were protonated, by addition of hydrochloric acid, to form the tricharged cation $\text{H}_3\text{II.6}^{3+}$. Further addition of aminoacids resulted in a general decrease of the absorption profile as result of the precipitation process. We speculate that the less soluble host-guest complex of the general formula $\text{HAA}^+ \cdots \text{H}_3\text{II.6}^{3+}$ (where HAA^+ is the protonated aminoacid molecule) formed in solution would precipitate as the concentration of aminoacid is increased. Identical results were obtained for glycine, alanine and valine.

Temperature dependence of ^{57}Fe -Mössbauer spectra for ferrocene-terpyridine systems

The Mössbauer Spectra for **II.4** and FTFC1_2 are shown in figure 9. The room temperature spectrum for **II.4** is typical for a ferrocene derivative and consists of a large and clear doublet. The IS value of 0.43 mm/s is similar (within the error limits) to the parent ferrocene, while the QS decreased by 0.22 mm/s (QS = 2.17 mm/s). This is a result of the electron withdrawing effect of the carboxylic substituent which increases the symmetry of the electron environment on the iron nucleus, by removing electron density from the cyclopentadiene ring and consequently from Fe d_{z^2} , d_{xz} , d_{yz} orbitals. The QS is even lower than for ferrocene-carboxylic acid [13], which suggests an additional effect of the terpyridine group. The spectrum of FTFC1_2 comprises two partially overlapped doublets attributed to the two carboxyferrocenes (IS = 0.44 mm/s, QS = 2.21 mm/s) and $[\text{Fe}(\text{tpy})_2]^{2+}$ component (IS = 0.21 mm/s, QS = 1.05 mm/s). All iron nuclei are low-spin ($S=0$) iron (d^6), but a more symmetrical pseudo-octahedral N_6 coordination results in a lower quadrupole splitting for $[\text{Fe}(\text{tpy})_2]^{2+}$ compared to ferrocene.

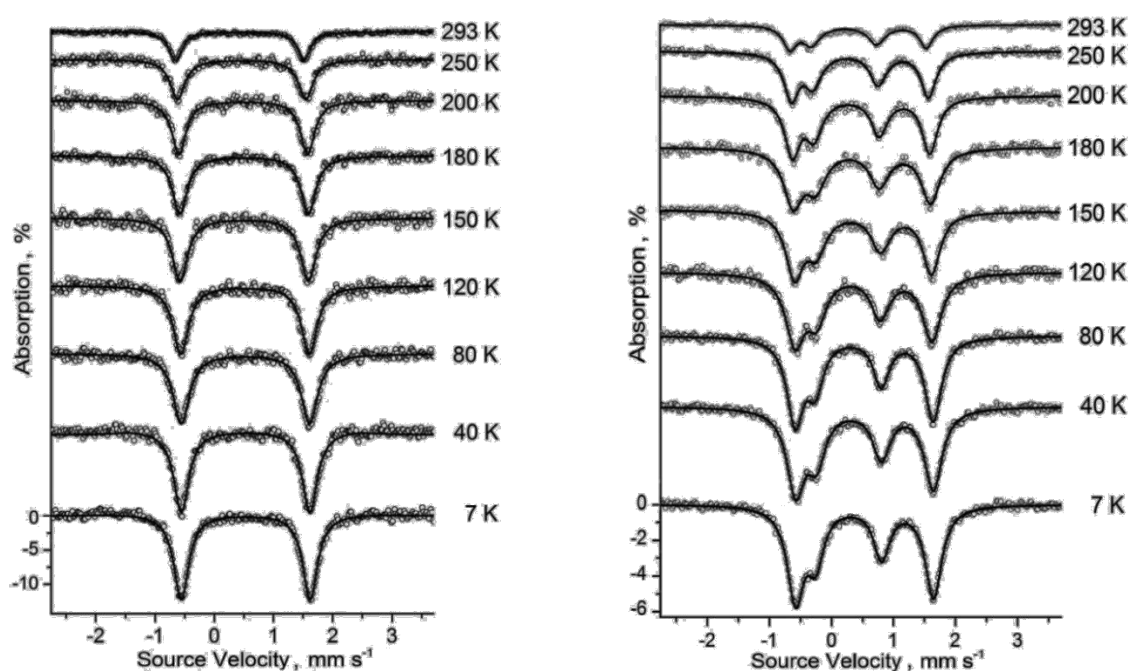


Fig. 9. The Mössbauer spectra for **II.4** (left) and FTFC1_2 (right) over 7-293 K temperature range.

The temperature dependence of the Debye-Waller factor of the Mössbauer spectra gives information on the vibration of atom in the molecule and of molecule in the crystal. The Debye temperature (θ_D) can be determined and used for comparison of forces that bind an atom in the molecule and crystal lattice [14]. With decreasing the temperature a strong increase of the absorption for the Fc was observed, less pronounced for the $[\text{Fe}(\text{tpy})_2]^{2+}$ nucleus, as result of vibration diminution for the examined atom in the crystal lattice. Plots of $\ln f'$ versus T allow us to calculate the Debye temperature from the slope of the line $\Delta(\ln f')/\Delta T$ [15]. The plot of $\ln f'_T/f'_{7K}$ versus T for **II.4** is linear over the temperature range 80 - 200 K and has a slope of $(4.0 \pm 0.3) \times 10^{-3}$ which corresponds to $\theta_D = (184 \pm 14)$ K. This value is somehow higher compared to that of parent ferrocene $\theta_D = (173 \pm 10)$ K. For the **FTFCl₂** two linear regressions were obtained for Fc and $[\text{Fe}(\text{tpy})_2]^{2+}$ nuclei, which gave $\theta_D = (180 \pm 17)$ K and $\theta_D = (218 \pm 15)$ K. The higher Debye temperature for the latter is suggesting a more rigid N₆ bonding of Fe atom by the two terpyridine molecules compared to the ferrocene "sandwich" structure.

2.2. Synthesis, molecular structure and properties of a ferrocene-based difluoropyrrolo-oxaborole derivative [6]

In attempts to prepare a bis(BODIPY)ferrocene derivative we found that the bis(ketopyrrole) derivative **FKP** was produced instead and could be converted readily to the BF₂ adduct, **FBF**. At first our interest was to see if the bis(BODIPY)ferrocene derivative can be obtained by using 1,1'-ferrocenedicarbaldehyde. The dipyrromethane derivative **II.9** is known [16] and was prepared without much problem in 70 % yield (Figure 10). All attempts in our hands to oxidise **II.9** and chelate two BF₂ units to the dipyrromethane groups failed.

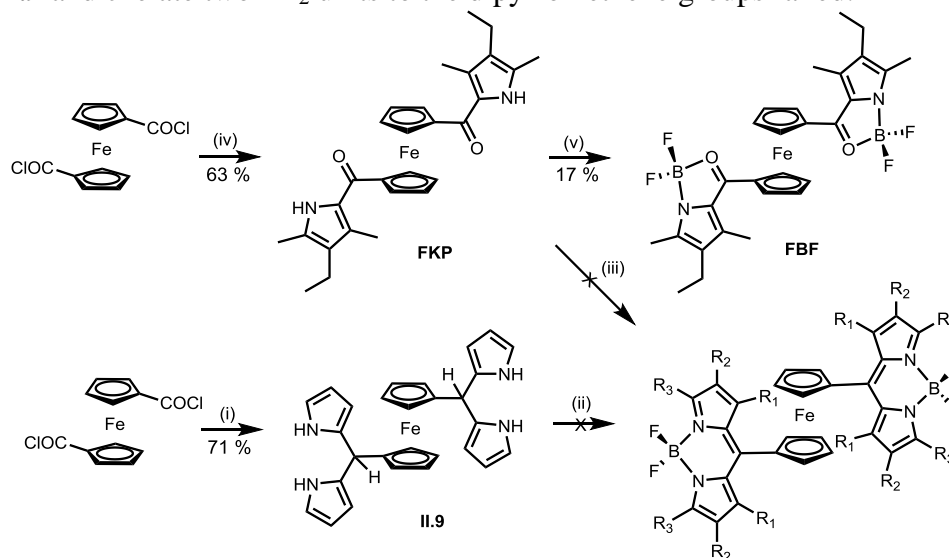


Fig. 10. Reagents and conditions: (i) pyrrole, TFA; (ii) DDQ or p-chloranyl or activated MnO₂; (iii) 3-ethyl-2,4-dimethylpyrrole, Et₃N, BF₃·OEt₂; POCl₃, 3-ethyl-2,4-dimethylpyrrole, Et₃N, BF₃·OEt₂; (iv) 3-ethyl-2,4-dimethylpyrrole; (v) Et₃N, BF₃·OEt₂.

Reaction of 1,1'-ferrocenedicarbonyl chloride with 3-ethyl-2,4-dimethylpyrrole in dichloromethane produced the half-way product - the ferrocene bis(2-ketopyrrole) derivative

FKP, and not the expected bis(dipyrromethene) compound. The 2-ketopyrrole compound reacted with $\text{BF}_3 \cdot \text{Et}_2\text{O}$ to produce the bis(difluoropyrrolo-oxaborole) compound, **FBF**, as a red / brown solid which was characterised by X-ray crystallography. The compounds were characterised by ASAP/APCI-FTMS and NMR spectroscopy including ^1H , $^{13}\text{C}\{^1\text{H}\}$, ^{11}B and ^{19}F nuclei.

As part of characterisation of the final compound and precursors, single crystals were grown for compounds **II.9**, **FKP** and **FBF**, and were subjected to X-ray diffraction analysis. The structures of **FKP** and **FBF** confirmed their identity and are shown in figure 11.

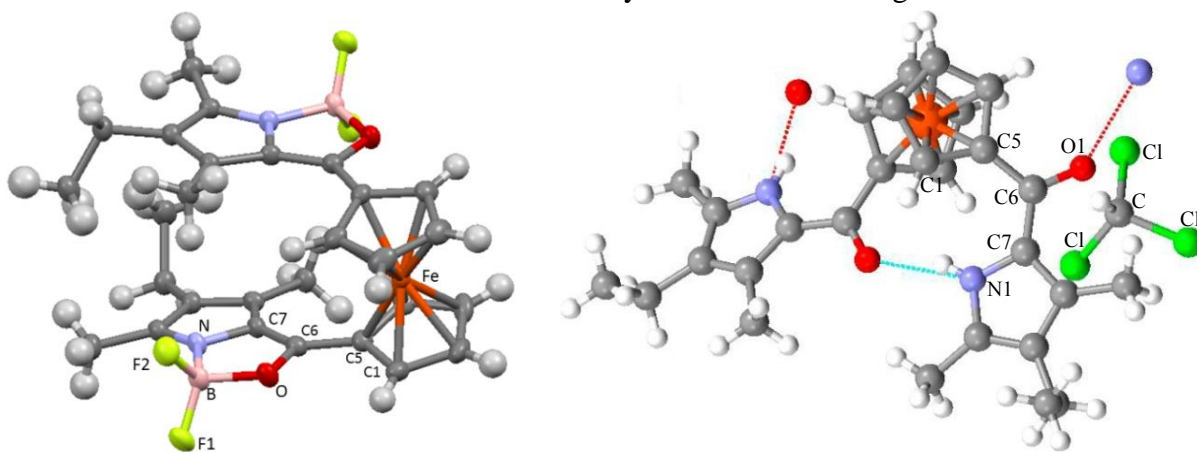


Fig. 11. Crystallographically determined molecular structures for **FBF** (left) and **FKP** with chloroform incorporated molecule (right).

Intramolecular hydrogen bond, $\text{N} - \text{H} \cdots \text{O}$, between a pyrrole and ketone on the two cyclopentadienyl (Cp) rings in **FKP** ($\text{N} - \text{O}$ distance 2.783 Å, $\text{N} - \text{H} - \text{O}$ angle 160.3°) twists the pyromethanone groups out of conjugation with their Cp rings by different amounts (dihedral angles 48.5° and 30.3°). The other $\text{N} - \text{H} \cdots \text{O}$ hydrogen bond is intermolecular linking the molecules in chains. The second point to note is the incorporation of a chloroform solvent molecule.

The compound **FBF** crystallises in the orthorhombic space group Pbcn. The asymmetric unit comprises half the molecular structure, the iron atom lying on a crystallographic twofold rotation axis. The geometry at the boron centre is close to tetrahedral. The two difluoropyrrolo-oxaborole groups are arranged tail-to-tail and are partially eclipsed. The torsion angle $\text{C1} - \text{C5} - \text{C6} - \text{O}$ is only 8.0° meaning the Cp ring and the pyrroloxaborole group are almost coplanar.

Temperature dependence of ^{57}Fe -Mössbauer spectra

The isomer shift and large quadrupole splitting for the clear doublet of **FKP** and **FBF** are typical for low-spin iron (d^6) ferrocene derivatives. The relatively low quadrupole splitting for the diketones compared with that of Fc are typical for conjugated electron-withdrawing substituents which increase the symmetry of the electron environment on the iron nucleus by removing electron density from the cyclopentadienyl rings [17]. The lower value for **FBF** compared with that of **FKP** is explained by the higher coplanarity of the electron-withdrawing substituents with the cyclopentadienyl rings, which ensures better overlap of π orbitals and an additional

withdrawing effect of the BF_2 group. Plots of $\ln(f'_T/f'_{7K})$ vs. T are linear over the temperature range 80 K to 200 K and the θ_D value for ferrocene was estimated at 173 K. As the relative absorption of **FBF** at room temperature has only a minor decrease compared with the parent ferrocene it was taken as being a very close value. The slope for the relative absorption of **FKP** is greater than that of the parent ferrocene. The calculated θ_D value is about 139 K. The lower Debye temperature for **FKP** compared with ferrocene and **FBF** suggests there are weaker intermolecular interactions or weaker Fe-Cp bonding.

DFT molecular modelling

Mulliken charges were calculated for the X-ray structures of **FBF** and **FKP** using DFT (B3PW91) and the 6-31G (3df) basis set. The first point to note is the increase in positive charge at the iron centre for **FBF** (+0.677) compared with that in **FKP** (+0.647). Because **FBF** is C_2 symmetric, the summation of Mulliken charges for carbon atoms at each Cp ring is identical (-0.739) and less than values for the Cp rings in compound **FKP** (-0.850, -0.874). There appears to be a slight extra build-up of negative charge (-0.024) on the one Cp ring for compound **FKP**. It is clear from the structure that this Cp ring and the difluoropyrrolo-oxaborole are more conjugated since the dihedral angle is only 11.9° compared with 40.9° at the other Cp site. The corresponding dihedral angle for **FBF** is only 8.0° meaning any conjugation is maximised for this system but it also contains the electron-withdrawing BF_2 unit.

Electrochemistry and absorption spectroscopy

The cyclic voltammogram of **FKP** (Figure 12) revealed a reversible wave at +0.31 V vs. Fc^+/Fc , and an irreversible wave at -2.38 V vs. Fc^+/Fc . Complexation of **FKP** with BF_2 causes a series of changes to the redox behaviour of **FBF**. The redox potential for the ferrocene is anodically shifted to +0.66 V vs. Fc^+/Fc and two quasi-reversible waves can be observed at -1.54 and -1.84 V vs. Fc^+/Fc .

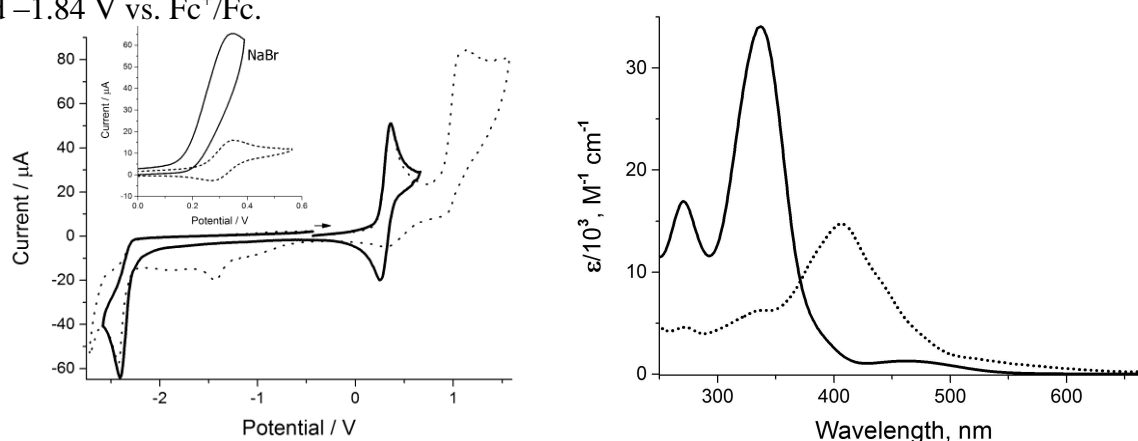


Fig. 12. Left: Cyclic voltammogram recorded for **FKP** in acetonitrile vs. Fc^+/Fc . Insert shows the changes induced by addition of NaBr. Right: Room-temperature UV-Vis absorption spectra for **FKP** (solid line) and **FBF** (dotted line) in acetonitrile.

It was noted that the ferrocene redox behaviour is irreversible in **FBF**, implying that a decomposition pathway is introduced for the ferrocenium ion. Considering that an electrophilic

centre is created in close proximity to a polarised B – F bond, nucleophilic attack of a fluorine atom at the ferrocenium is one possible breakdown mechanism. To support this idea, NaBr was added to a solution of **FKP** in MeCN, which resulted in complete loss of reversibility of the ferrocene couple. Additionally, the irreversible anodic wave shifts to a lower potential, affording a very similar voltammogram to that of **FBF** alone.

The room-temperature electronic absorption spectrum for **FKP** (Figure 12) consists of a band in the near-UV region at $\lambda_{\text{max}} = 271 \text{ nm}$ ($\epsilon_{\text{max}} = 1.7 \times 10^4 \text{ M}^{-1} \text{ cm}^{-1}$) and a moderately strong narrow band at $\lambda_{\text{max}} = 337 \text{ nm}$ ($\epsilon_{\text{max}} = 3.4 \times 10^4 \text{ M}^{-1} \text{ cm}^{-1}$). A much less intense broad band can also be observed in the visible region at $\lambda_{\text{max}} = 462 \text{ nm}$ ($\epsilon_{\text{max}} = 1.3 \times 10^3 \text{ M}^{-1} \text{ cm}^{-1}$). Chelation with BF_2 changes the absorption profile entirely (Figure 12), resulting in a considerably broader, but weaker band in the visible region at $\lambda_{\text{max}} = 407 \text{ nm}$ ($\epsilon_{\text{max}} = 1.4 \times 10^4 \text{ M}^{-1} \text{ cm}^{-1}$) with a shoulder at 339 nm. The intensity of the band at $\lambda_{\text{max}} = 272 \text{ nm}$ ($\epsilon_{\text{max}} = 7.5 \times 10^3 \text{ M}^{-1} \text{ cm}^{-1}$) is considerably less.

3. FERROCENE-PORPHYRIN CONJUGATES

Numerous reports are available discussing the different processes in DSSC and trying to identify the “bottle-neck” which is limiting the efficiency of manufactured devices [18]. There is one argument that charge must be shifted away from the semiconductor surface rapidly to generate long-lived charge-separated species [19] and avoid the charge recombination which was estimated to occur in the range of $100 \mu\text{s} - 1 \text{ ms}$ [20].

3.1. Synthesis, properties of a *meso*-tris-ferrocene appended Zinc(II) porphyrin and evaluation of its dye sensitised solar cell performance [7]

The most basic porphyrin based molecular system incorporating *meso*-ferrocene units is exemplified in figure 13. The cartoon represents the basic working of the system following excitation of the porphyrin moiety, where process 1 is oxidation of a ferrocene by the excited state and process 2 is the charge recombination. It could be argued that if charge injection from the porphyrin excited state (process 3) competed with process 1 then the system would operate.

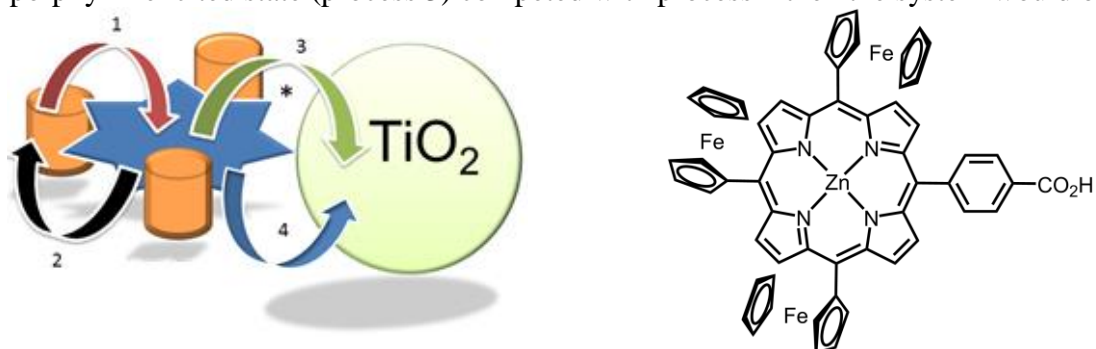


Fig. 13. Left: Simple cartoon showing potential electron transfer pathways following excitation of the zinc(II) porphyrin. Brown cylinders represent Fc units, blue star represents porphyrin macrocycle, arrows represent electron transfer pathways: 1. charge separation; 2. charge recombination; 3. electron injection from zinc-porphyrin excited state; 4. electron injection from porphyrin radical anion.

Right: Tris-ferrocene zinc(II) porphyrin **F3P** containing the carboxylic acid anchoring unit.

Alternatively, if electron injection from the porphyrin anion (process 4) was fast and efficient then the energy wasting recombination process 2 would become less significant. We are, of course, not considering the recombination process involving back electron transfer from the conduction band of the TiO₂.

Two strategies were involved in order to obtain **III.4**: condensation of methyl 4-formylbenzoate and three equivalents of ferrocenecarboxaldehyde with pyrrole in the presence of trace acid to give target compound in 14 % yield as a purple solid; the use of the preformed 5-ferrocenyldipyrromethane **III.3** [21] and its condensation with **III.2** and ferrocenecarboxaldehyde with a slightly improved yield of 18 %. ¹H NMR spectra recorded for samples of **III.4** prepared by both methods were identical. A *cis* isomer of bisferrocenyl porphyrin was isolated as well, namely 5,10-bisferrocenyl-15,20-bis(4-methyl benzoate)porphyrin **III.5** according to ¹H NMR spectrum. The final two reactions of incorporation of zinc(II) into the porphyrin ring to obtain intermediate **III.6** and ester group hydrolysis worked in high yields to afford the desired compound Zn(II) 5,10,15-trisferrocenyl-20-(4-carboxyphenyl) porphyrin **F3P**.

Full characterisation of **F3P** by IR, MALDI mass ($m/z = 1044$) and ¹H, ¹³C{¹H} and DEPT-135° NMR spectra, as well as two-dimensional homo-(¹H/¹H COSY-45°) and heteronuclear (¹H/¹³C HSQC and HMBC) correlation spectra corroborated the expected structure.

DFT molecular orbital calculations

The MO picture from the B3PW91 6-31G(d) calculation is shown in figure 14. It can be seen that HOMO is predominantly localised on the three ferrocene moieties, whereas the HOMO-1 is exclusively porphyrin based. The MOs HOMO-2 to HOMO-6 are entirely ferrocene centred. The LUMO and LUMO+1 are degenerate and porphyrin-based π* orbitals in agreement with Gouterman's four orbital model [22]. Both orbitals are well separated in energy from the LUMO+2 which resides on the *meso*-benzoic acid group. Very crudely the HOMO-LUMO gap represents ferrocene-to-porphyrin charge transfer, the energy difference being 2.59 eV (479 nm).

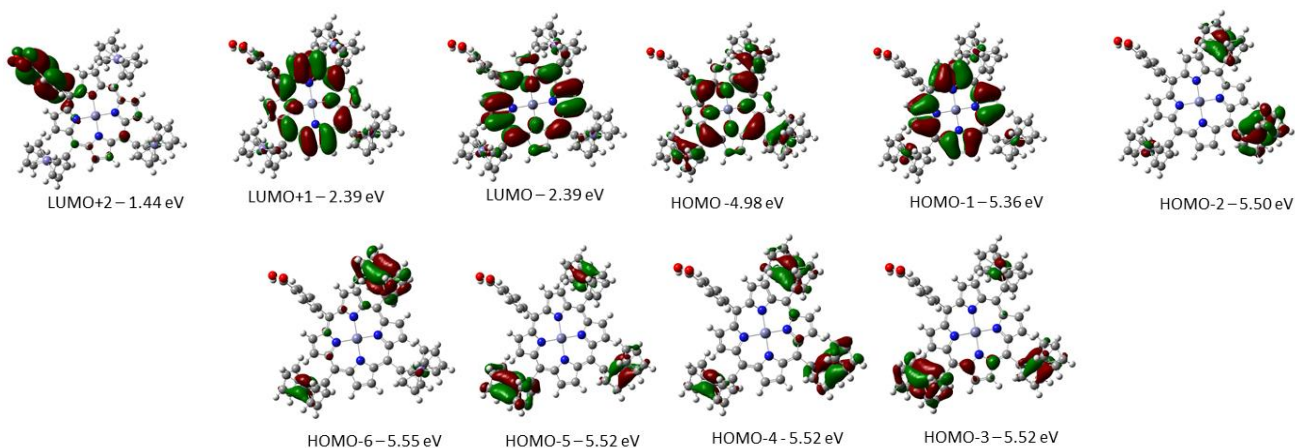


Fig. 14. Selected molecular orbitals pictures and their corresponding energy for **F3P**, calculated by DFT (B3PW91) and using a 6-31G(d) basis set.

Electrochemistry, electronic absorption and ^{57}Fe Mössbauer spectroscopy

The cyclic voltammogram for **F3P** in dry THF (Figure 15) showed a clear quasi-reversible wave at +0.04 V vs. Fc^+/Fc , which is associated with redox at the ferrocene sites. At a more positive potential an irreversible wave is observed at +1.1 V vs. Fc^+/Fc which is porphyrin-based oxidation. Upon scanning to negative potentials two quasi-reversible one-electron waves are seen at -1.87 V and -2.20 V vs. Fc^+/Fc and are again associated with redox at the porphyrin site.

The room temperature electronic absorption spectrum for **F3P** in chloroform is shown in figure 15. The spectrum comprises a strong Soret B-band at 431 nm ($1.6 \times 10^5 \text{ M}^{-1} \text{ cm}^{-1}$) and a much weaker Q-band at 661 nm ($1.7 \times 10^4 \text{ M}^{-1} \text{ cm}^{-1}$), typical of a divalent metalloporphyrin. The weak band at 310 nm ($2.1 \times 10^4 \text{ M}^{-1} \text{ cm}^{-1}$) may be assigned to the lesser discussed porphyrin N-band. The Soret band also contains a ferrocene-to-porphyrin charge transfer band in the region of ~ 490 nm which improves the light harvesting in the visible spectrum.

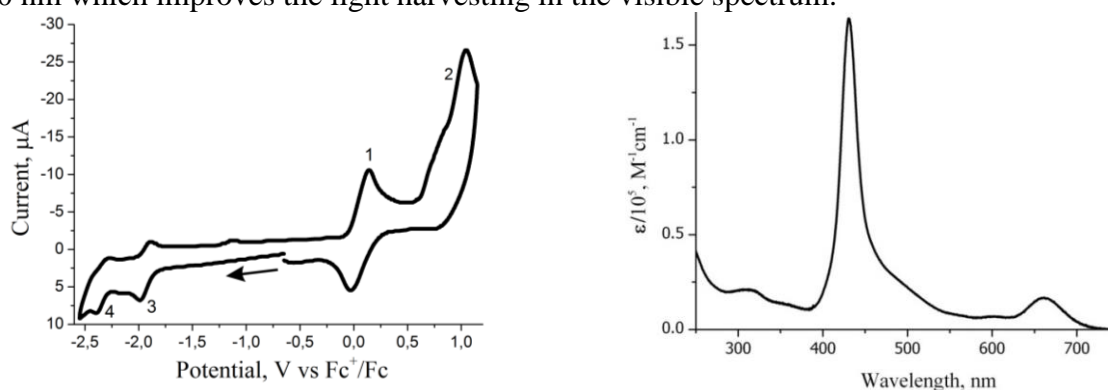


Fig. 15. Left: Cyclic voltammogram for **F3P** in THF (0.2 M TBABF₄) at a glassy carbon working electrode. Right: Room temperature UV-Vis absorption spectrum for **F3P** in chloroform.

The room temperature Mössbauer spectrum for **F3P** showed IS and large QS for the clear doublet typical for low-spin iron (d^6) ferrocene derivatives. The comparison of **F3P** and parent ferrocene shows that the porphyrin core has no major influence on the electron density at the iron nucleus, despite the close proximity of the ferrocene and porphyrin groups.

Evaluation of excited state deactivation for DSSC application

The plot of photocurrent density versus voltage (under standard AM 1.5 global sunlight at 1000 W m^{-2} and a temperature of 298 K) for **F3P** showed the short circuit current density (J_{SC}) to be 0.068 mA cm^{-2} , the open circuit voltage (V_{OC}) of 283 mV, the fill factor (FF) of 0.42 and the power conversion efficiency was evaluated to be 0.0081 %. The experiment was repeated in darkness and proved the photovoltaic nature of the effect.

The excited-state property for **F3P** was elucidated using femtosecond pump-probe spectroscopy in THF (Figure 16).

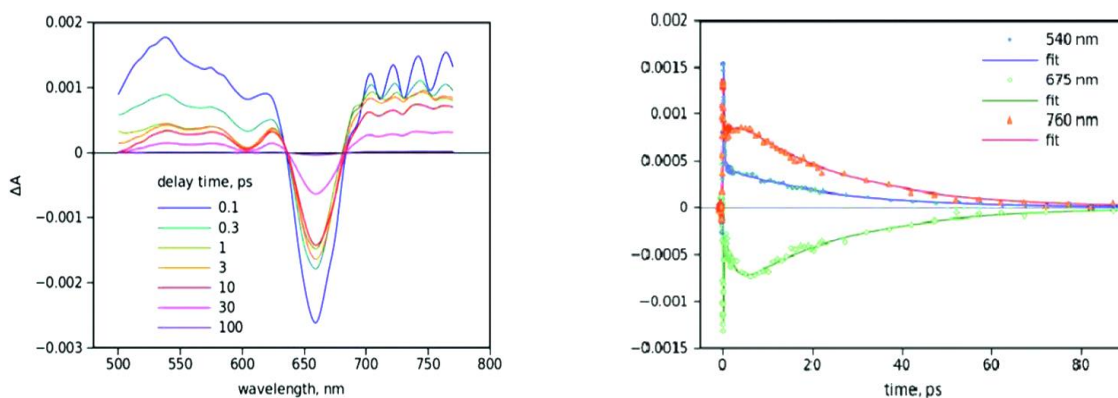


Fig. 16. Selected transient absorption spectra recorded after excitation of **F3P** in THF with a 70 fs laser pulse delivered at 480 nm (left). Transient absorption decay profiles of **F3P** in THF at selected wavelengths (right). Symbols are measured data and lines are fit curves.

The excitation with a 70 fs laser pulse at 480 nm resulted in an almost instantaneous bleach in the region around 660 nm corresponding to the Q-bands of the porphyrin and a broad profile to the low energy side of this bleach assigned to the zinc-porphyrin radical anion [23]. The charge separation time constant was estimated at 190 fs, while the charge recombination process though slower by comparison is still extremely rapid and reforms the ground state in $\tau = 24$ ps. The behaviour for **F3P** attached to TiO_2 was also measured and compared to a control compound containing phenyl groups instead of the ferrocene moieties (**ZnTFP**). The excited state spectroscopic data for **F3P** attached to TiO_2 shows unequivocally that the dye is rather poor at injecting electrons into the conduction band of the semiconductor TiO_2 . Generally electron injection into TiO_2 is extremely fast and in the order of 300 fs [24]. For the control compound the excited state porphyrin injects electrons in around 130 fs. Assuming this latter value is the same for **F3P** the maximum yield of electrons into the TiO_2 conduction band is only 60 %. Another significant finding is electron injection from the porphyrin anion to the TiO_2 does not take place in the lifetime of the CS state (29 ps). These results suggest that direct coupling of donors and porphyrin should be avoided in the design of DSSC sensitisers as the injection from the rapidly generated porphyrin anion onto the TiO_2 surface does not occur. There is the additional argument that ferrocenium / ferrocene may not be conducive for coupling to the $\text{Co}^{(\text{II/III})}$ electrolyte redox relay because of slow electron exchange kinetics [25].

3.2. Electrocatalytic hydrogen production using Palladium(II) and Copper(II) *meso*-tetraferrocenyl porphyrin complexes

Cu(II) and Pd(II) *meso*-tetraferrocenylporphyrines (**CuTFP** & **PdTFP**) shown in figure 17 were employed as catalysts for electrochemical proton reduction in DMF using trifluoroacetic acid (TFA) or triethylamine hydrochloride (TEAHCl) as acids. **CuTFP** [26] and **PdTFP** were obtained by complexation of **H₂TFP** with Pd(II) acetate or Cu(II) acetate in moderate yields. All our attempts to obtain crystals suitable for X-ray analysis failed for complexes [26], but the structure of **H₂TFP** was repeatedly [27] obtained (Figure 17), and confirmed its identity.



Fig. 17. Left: The structure of ferrocene-porphyrin compounds discussed in the text.
Right: Crystallographically determined molecular structure for **H₂TFP**

Electrochemistry, electronic absorption and UV-Vis spectroelectrochemistry

The cyclic voltammogram for **PdTFP** in DMF consists of redox patterns for a porphyrin and ferrocene moieties (Figure 18). Upon scanning to positive potentials a quasi-reversible wave at +0.08 V vs. Fc^+/Fc is seen, associated with ferrocene couple, and an irreversible wave of porphyrin-based oxidation is observed at +0.93 V vs. Fc^+/Fc . The reduction side of the voltammogram shows two quasi-reversible one-electron waves at -1.72 V and -2.21 V vs. Fc^+/Fc and are again associated with redox at the porphyrin site. The room temperature electronic absorption spectra for **H₂TFP**, **CuTFP** and **PdTFP** in THF comprise a strong Soret B-band and one weaker Q-band for metalated porphyrins, while two Q-band were found for **H₂TFP**.

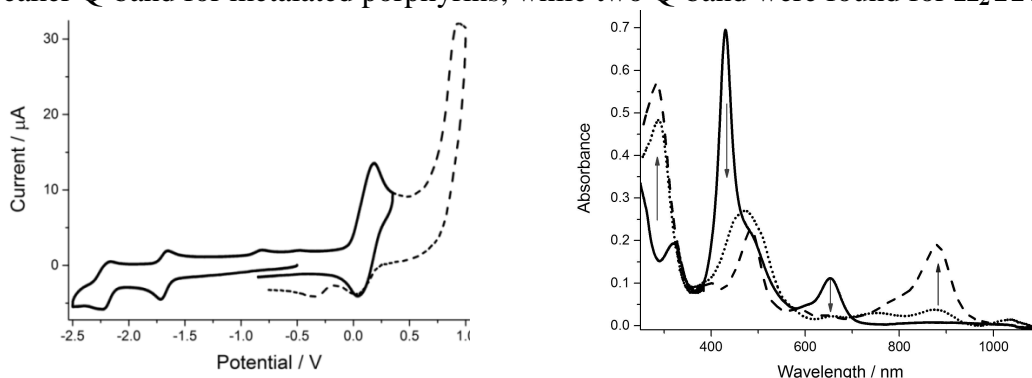


Fig. 18. Left: Cyclic voltammogram recorded for **PdTFP** in DMF vs Fc^+/Fc . Right: UV-Vis absorption spectra for **PdTFP** in THF: at the start (solid), after reduction at -1.3 V (dotted) and -1.7 V (dashed).

Application of a negative potential of -1.3 V to the working electrode in an OTTLE produced a drastic decrease in the Soret band and the appearance of a red-shifted broad band (Figure 18). The Q-band almost fully disappeared and three new weak and broad bands appeared at 750, 875 and 1035 nm. The spectrum is typical for a porphyrin mono-anion **MTFP⁻** [28] so the first reduction process is porphyrin centred. Further reduction at -1.7 V resulted in a narrowing and slight decrease in the Soret band. In the low-energy side of the spectrum is witnessed a substantial increase in the absorption at 880 nm. The formation of the porphyrin dianion **MTFP²⁻** would result in disappearance of the near-IR bands, but a similar strong band at 825 nm was reported to correspond to the Zn(II) tetraphenylphlorin monoanion obtained both by chemical [28] and electrochemical reduction [29] of Zn(II) tetraphenylporphyrin, and 830 nm for a metal

free tetraphenylphlorin [30]. It means that the second reduction results in formation of **MTFP**²⁻ followed by protonation to give the phlorin anion **MTFPH**⁻.

Electrocatalytic proton reduction

The addition of trifluoroacetic acid to **PdTFP** or **CuTFP** gave rise to a new catalytic wave (Figure 19) in cyclic voltammetry experiment at -2.0 V vs Fc⁺/Fc, representative for a diffusion limited process. Its amplitude constantly increases with addition of acid up to 200 eq of TFA for **PdTFP** and 500 eq of TFA for **CuTFP**, corresponding to a turnover frequency of 10⁴ s⁻¹ order. An overpotential of -1.0 V was estimated as described by Artero and coworkers [31].

The metal-free, Zn(II) and Co(II) **TFP** showed no catalytic activity in identical conditions, while Ni(II) **TFP** showed weak current response at a higher potential. The use of a weaker acid TEAHCl as the proton source resulted in no catalytic activity for **PdTFP**, while **CuTFP** showed similar behaviour as for TFA (Figure 19).

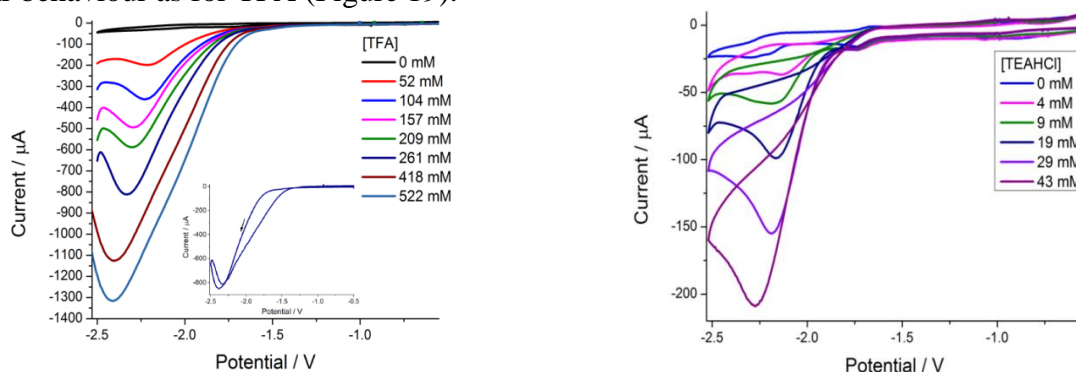


Fig. 19. Selected cyclic voltammograms of 1 mM of **CuTFP** at a glassy carbon electrode in DMF in the presence of increasing quantities of TFA (left) and TEAHCl (right).

Copper(II) complex of tetraphenylporphyrin (**TPP**) was reported to be a non-active hydrogen evolving catalyst (with TEAHCl or CHF₂COOH), [32] and we found that both **CuTPP** and **PdTPP** are far less active than their ferrocene analogue when using TFA as the acid source. The overpotential is shifted to a more negative value by around 200 mV and the catalytic rate in DMF/TFA is slower with an order of magnitude. The higher catalytic activity of ferrocene substituted porphyrins could be attributed to stabilization of protonated intermediates by increasing electron density on the porphyrin periphery, which is suggested from Mössbauer spectroscopy data. Formation of *meso*-protonated porphyrin intermediate was seen in spectroelectrochemical experiments so a catalysis mechanism based on initial phlorin formation is highly probable. It was previously shown that phlorins can undergo dehydrogenation in the presence of a proton source (HCl, methanol) so that the parent porphyrin is generated [33]. Another explanation of ferrocene role is the stabilization of phlorins by steric hindrance of parent porphyrin, previously proposed for other porphyrin systems [34].

Continuous flow rig with in-line GC analysis [35] was used to detect the molecular hydrogen produced during electrocatalytic proton reduction in DMF in the presence of TFA and TEAHCl,

applying a potential of -1.5 V vs Saturated Calomel Electrode at Glassy Carbon working electrode. Undoubtedly the presence of 0.1 mM of the catalyst greatly increased the amount of electroreduced protons, as indicated by the GC analysis. Using 0.1 mM of **CuTFP** in DMF solution of 50 mM TFA with 0.1 M TBABF₄ as supporting electrolyte resulted in electrocatalytic production of H₂ with a 68 % Faradaic yield (Figure 20). A Faradaic efficiency of 70 % was obtained by the use of **PdTFP** catalyst, but less protons were reduced in the same period of time. As only **CuTFP** showed electrocatalytic behaviour in CV experiments when TEAHCl was employed as proton source, it was used to generate H₂ from this weaker acid (Figure 20). As expected, the catalysis process is slower for this acid at the same concentration C_M = 50 mM and identical applied potential, as result of higher pK_a = 9.2 (pK_a = 6 for TFA) [31, 36]. A Faradaic efficiency of about 73 % was obtained.

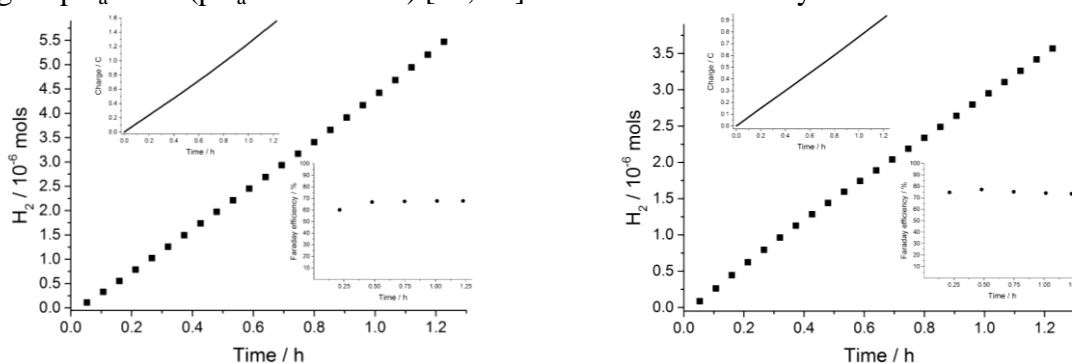


Fig. 20. Electrocatalytic hydrogen production vs time, for solution of DMF containing: left - 50 mM TFA and 0.1 mM **CuTFP**; right - 50 mM TEAHCl and 0.1 mM **CuTFP**. The inserts are showing plots of charge vs time (left) and Faradaic yield vs time (right).

4. EXPERIMENTAL SECTION

In the first half of this chapter a detailed information on the instruments used to study the materials obtained within this work is given, together with the software used to run the apparatus, process data and perform quantum-chemical calculations. The second part is providing the reader with details on the reaction conditions employed to obtain the compounds discussed in Chapters 2 and 3, and X-ray crystallographic data. Using the twenty seven synthesis procedures described in the above chapter, twenty six products were synthesized, from which fourteen products are new ferrocene and porphyrin based derivatives. Nine products are heteronuclear homo- and heteroleptic coordination compounds of ferrocene based ligands with boron(III), iron(II), cobalt(II), nickel(II), copper(II), zinc(II), ruthenium(II) and palladium(II) atoms. The structure of compounds was confirmed by IR, NMR, atomic absorption, mass spectrometries, elemental analysis and X-ray crystallography. In order to study and explain the physico-chemical properties of products a number of modern methods were used, namely: Mössbauer, UV-Vis absorption spectrometries, cyclic voltammetry, UV-Vis spectroelectrochemistry, ultrafast transient absorption Pump-Probe spectrometry and computer assisted DFT calculations. Application potential of the final products was studied in a number of systems, including Dye Sensitised Solar Cells and electrocatalytic proton reduction cell.

OVERALL CONCLUSIONS AND RECOMMENDATIONS

1. A new method for desymmetrization of the ferrocene was elaborated based on KMnO_4 oxidation of 1,1'-ferrocenedicarboxaldehyde. The two resulting products were used to obtain compounds **II.4** – **II.6**. Interestingly, the product **II.4** showed to be light sensitive and more detailed study showed a light induced degradation of ferrocene unit to form the $[\text{Fe}(\text{tpy})_2]^{2+}$ complexes. As result the complex **FTF**²⁺ was isolated and studied with various methods, including Mössbauer spectrometry. It was found that the Debye temperature has the values: (184 ± 14) and (180 ± 17) K for ferrocene components of **II.4** and **FTFCl**₂ and $\theta_D = (218\pm 15)$ K for $[(\text{Fe}(\text{tpy})_2)]^{2+}$ unit. The mechanism leading to formation of derivative **II.5** is a fascinating example of the organic / organometallic chemistry complexity. The cyclohexenone ring contains a chiral centre showing the potential of generating materials for applications in asymmetric catalysis. At the same time, compound **II.6** could find application in visual α -aminoacids recognition by precipitation of host-guest complexes in acidified aqueous solutions.

2. In the attempt to obtain 1,1'-ferrocene bis(BODIPY), the half way ketopyrrole product and its BF_2 complex were obtained. UV-Vis absorption, Mössbauer spectrometries, cyclic voltammetry and spectroelectrochemistry, combined with DFT calculations, were used in order to characterize their properties. Unfortunately the poor irreversible electrochemistry witnessed for the pyrroloxaborole derivative **FBF** does preclude its use as a useful redox reporter. On the other hand, compound **FKP** may be more suitable by using the chelating properties of the ketopyrrole group, and the binding of groups with nucleophilic character. Noting that the absorption profile for **FBF** stretches well into the red region, the compound may have more application as a dark-state energy transfer quencher for fluorophores which emit between 500 and 600 nm.

3. In the preparation of the trisubstituted ferrocene-based porphyrin derivative it would appear that the “one-pot” stoichiometry-correct reaction works as well as the preorganised method starting from a ferrocene-dipyrrromethane precursor. The only advantage of the second method is the slightly easier purification of the final product. Our results clearly show that only direct photoinjection from the porphyrin excited state is relevant for the outlined ferrocene–porphyrin derivatives. Hence in the design of porphyrin-based systems for DSSC applications strongly coupled donor-acceptor pairs should be avoided.

4. Cu(II) and Pd(II) tetraferroceneporphyrines were synthesized and used as catalysts for electrochemical proton reduction. The cyclic voltammetry experiments showed that electrocatalysis occurs when proton source is added (TFA or TEAHCl) at a moderate potential. The formation of phlorin intermediate was proved by UV-Vis spectroelectrochemistry. Performing bulk electrolysis with concomitant continuous flow rig with in-line GC analysis was used to detect qualitatively and quantitatively the molecular hydrogen produced. Certainly the introduction of ferrocene enhanced the electrocatalytic activity of porphyrin molecules, compared with tetraphenyl analogues. A cooperative ferrocenyl and metal influence is suggested, resulting in increased electron density on the periphery of porphyrin and steric hindrance effect. Hence, while most of the literature examples are based on the metal redox chemistry, this is an example of carbon-centred electrocatalysis of proton reduction.

REFERENCES:

1. Phougat N. et al. Metal porphyrins as electrocatalysts for commercially important reactions. In: Transition Metal Chemistry, 2003, nr. 28, p. 838-847.
2. Bhugun I., Lexa D., Saveant J.-F. Catalysis of the Electrochemical Reduction of Carbon Dioxide by Iron(0) Porphyrins. Synergistic Effect of Lewis Acid Cations. In: J. Phys. Chem., 1996, nr. 100, p. 19981-19985.
3. Bhugun I., Lexa D., Saveant J.-F. Homogeneous Catalysis of Electrochemical Hydrogen Evolution by Iron(0) Porphyrins. In: J. Am. Chem. Soc., 1996, nr. 118 (16), p. 3982-3983.
4. Blaser H.-U., Spindler F. Enantioselective Catalysis for Agrochemicals: The Case History of the DUAL MAGNUM® Herbicide. In: CHIMIA International Journal for Chemistry, 1997, nr. 51 (6), p. 297-299.
5. Benniston A.C., Sirbu D. et al. A simple method for desymmetrizing 1,1'-ferrocene dicarboxaldehyde. In: Tetrahedron Letters, 2014, nr. 55 (28), p. 3777-3780.
6. Benniston A.C., Sirbu D. et al. Synthesis, molecular structure and properties of a ferrocene-based difluoropyrrolo-oxaborole derivative. In: Eur. J. Inorg. Chem., 2014, nr. 36, p. 6212-6219.
7. Sirbu D. et al. Synthesis and properties of a meso- tris-ferrocene appended zinc(II) porphyrin and a critical evaluation of its dye sensitised solar cell (DSSC) performance. In: RSC Adv., 2014, nr. 4, p. 22733-22742.
8. Sirbu D. Temperature dependence of ^{57}Fe -mössbauer spectra for a $\text{Fe}_{\text{Fc}}^{\text{II}} - \text{Fe}_{\text{tpy}}^{\text{II}} - \text{Fe}_{\text{Fc}}^{\text{II}}$ trinuclear system. In: Chemistry Journal of Moldova. General, Industrial and Ecological Chemistry, 2015, nr. 10 (1), p. 84-88.
9. Turta C., Duca G., Marin I., Sirbu D. Chapter 3: Electrochemical Solar Cells Based on Pigments. In: Management of Water Quality in Moldova, SPRINGER, Series: Water Science and Technology Library, 2014, Vol. 69, p. 48-59.
10. Batsanov A.S. et al. Synthesis and Structure of Planar Chiral, Bifunctional Aminoboronic Acid Ferrocene Derivatives. In: Organometallics, 2007, nr. 26, p. 2414-2419.
11. Xiang J.-N. et al. An efficient approach to the synthesis of 1,3-diaryl-1,2,3,4-[4H]-tetrahydronaphthalene-2-carboxylic acids. In: Bioorg. Med. Chem., 1998, nr. 6, p. 695-700.

12. Lin Li et al. Synthesis, characterization and crystal structure of 6-ferrocenyl-2,4-dihydroxy-2,4-di(pyridine-2-yl) cyclohexanecarbonyl ferrocene. In: *Transition Met Chem*, 2008, nr. 33, p. 85-89.
13. Korecz L. et al. The Mössbauer investigation of some derivatives of ferrocenes. In: *Inorganica Chimica Acta*, 1974, nr. 9, p. 209-212.
14. Pingheng Z. et al. Temperature Dependence of the Mössbauer Effect on Prussian Blue Nanowires. In: *Hyperfine Interactions*, 2002, nr. 142, p. 601-606.
15. Herber R.H. *Chemical Mössbauer Spectroscopy*. New York: Plenum Press, 1984, p. 199-216.
16. Koszarna B., Butenschän H., Gryko D.T. The synthesis and properties of bis-1,1'-(porphyrinyl)ferrocenes. In: *Org. Biomol. Chem.*, 2005, 3, p. 2640-2645.
17. Clemance M.C., Roberts R.M.G., Silver J. Mössbauer studies on ferrocene complexes VIII. Diacetyl ferrocene-metal halide complexes. In: *Journal of Organometallic Chemistry*, 1983, nr. 247, p. 219-222.
18. Haque S.A. et al. Charge Separation versus Recombination in Dye-Sensitized Nanocrystalline Solar Cells: the Minimization of Kinetic Redundancy. In: *J. Am. Chem. Soc.*, 2005, nr. 127, p. 3456-3462.
19. Tian H. et al. A Triphenylamine Dye Model for the Study of Intramolecular Energy Transfer and Charge Transfer in Dye-Sensitized Solar Cells. In: *Adv. Funct. Mater.*, 2008, nr. 18, p. 3461-3468.
20. Richard L.W. et al. Electron Dynamics in Nanocrystalline ZnO and TiO₂ Films Probed by Potential Step Chronoamperometry and Transient Absorption Spectroscopy. In: *J. Phys. Chem. B*, 2002, nr. 106 (31), p. 7605-7613.
21. Narayanan S.J. et al. Synthesis of meso Ferrocenyl Porphyrins. In: *Synlett*, 2000, nr. 12, p. 1834-1836.
22. Gouterman M., Wagnière G. H. Spectra of porphyrins. In: *J. Mol. Spectrosc.*, 1963, nr. 11, p. 108-127.
23. Closs G.L., Closs L.E. Negative Ions of Porphin Metal Complexes. In: *J. Am. Chem. Soc.*, 1963, nr. 85, p. 818-819.
24. Hart A.S. et al. Porphyrin-Sensitized Solar Cells: Effect of Carboxyl Anchor Group Orientation on the Cell Performance. In: *ACS Appl. Mater. Interfaces*, 2013, nr. 5 (11), p. 5314-5323.

25. Feldt S.M. et al. Regeneration and recombination kinetics in cobalt polypyridine based dye-sensitized solar cells, explained using Marcus theory. In: *Phys. Chem. Chem. Phys.*, 2013, nr. 15, p. 7087-7097.
26. Nemykin V.N. et al. Metal-free and transition-metal tetraferrocenylporphyrins part 1: synthesis, characterization, electronic structure, and conformational flexibility of neutral compounds. In: *Dalton Trans.*, 2008, nr. 32, p. 4233-4246.
27. Nemykin V.N. et al. Long-Range Electronic Communication in Free-Base meso-Poly(Ferrocenyl)-Containing Porphyrins. In: *Inorg. Chem.*, 2010, nr. 49, p. 7497-7509.
28. Closs G.L., Closs L.E. Negative Ions of Porphin Metal Complexes. In: *J. Am. Chem. Soc.*, 1963, nr. 85, p. 818-819.
29. Lanese J.G., Wilson G.S. Electrochemical Studies of Zinc Tetraphenylporphin. In: *J. Electrochem. Soc.*, 1972, nr. 119 (8), 1039-1043.
30. Wilson G.S., Peychal-Heiling G. Electrochemical studies of tetraphenylporphin, tetraphenylchlorin, and tetraphenylbacteriochlorin. In: *Anal. Chem.*, 1971, nr. 43 (4), p. 550-556.
31. Fourmond V. et al. H₂ Evolution and Molecular Electrocatalysts: Determination of Overpotentials and Effect of Homoconjugation. In: *Inorg. Chem.*, 2010, nr. 49, p. 10338-10347.
32. Bhugun I., Lexa D., Saveant J.-F. Homogeneous Catalysis of Electrochemical Hydrogen Evolution by Iron(0) Porphyrins. In: *J. Am. Chem. Soc.*, 1996, nr. 118 (16), p. 3982-3983.
33. Krattinger B., Callot H.J. The first stable monocyclic phlorin free base. Preparation and X-ray structure determination of 5,21-dihydro-5,10,15,20,22-pentaphenylporphyrin (N-phenyl-meso-tetraphenylphlorin). In: *Chem. Commun.*, 1996, p. 1341-1342.
34. Inhoffen H.H. et al. Zur weiteren Kenntnis des Chlorophylls und des Hämins, XII. Elektrochemische Reduktionen an Porphyrinen und Chlorinen, IV. In: *Justus Liebigs Annalen der Chemie*, 1967, nr. 704 (1), p. 188-207.
35. Summers, P.A.; Dawson, J.; Ghiotto, F.; Hanson-Heine, M.W.D.; Vuong, K.Q.; Davies, E.S.; Sun, X.-Z.; Besley, N.A.; McMaster, J.; George, M.W.; Schröder, M. *Inorg. Chem.*, 2014, 53 (9), 4430-4439.
36. Fourmond V. et al. A nickel-manganese catalyst as a biomimic of the active site of NiFe hydrogenases: a combined electrocatalytical and DFT mechanistic study. In: *Energy Environ. Sci.*, 2011, nr. 4, p. 2417-2427.

THE LIST OF SCIENTIFIC PAPERS LINKED TO THE THESIS

Chapters in books:

Turta, C.; Duca, G.; Marin, I.; **Sirbu, D.** Chapter 3: Electrochemical Solar Cells Based on Pigments. In: *Management of Water Quality in Moldova*, SPRINGER, Series: *Water Science and Technology Library*, 2014, Vol. 69, p. 48-59.

Articles in scientific journals:

- in international journals rated ISI and SCOPUS:
 - **Sirbu, D.**; Turta, C.; Benniston, A. C.; Abou-Chahine, F.; Lemmetyinen, H.; Tkachenko, N. V.; Woodd, C.; Gibson, E. Synthesis and properties of a meso tris-ferrocene appended zinc(II) porphyrin and a critical evaluation of its dye sensitised solar cell (DSSC) performance. In: **RSC Advances**, 2014, V. 4 (43), p. 22733-22742
 - Benniston, A.C.; **Sirbu, D.**; Turta, C.; Probert, M.R.; Clegg, W. Synthesis, molecular structure and properties of a ferrocene-based difluoropyrrolo-oxaborole derivative. In: **Eur. J. Inorg. Chem.**, 2014, V. 36, p. 6212-6219.
 - Benniston, A.C.; **Sirbu, D.**; Turta, C.; Probert, M.R.; Clegg, W. A simple method for desymmetrizing 1,1'-ferrocenedicarboxaldehyde. In: **Tetrahedron Letters**, 2014, V. 55 (28), p. 3777-3780
 - **Sirbu, D.**; Turta, C.; Gibson, E.A.; Benniston, A.C. The Ferrocene Effect: Enhanced Electrocatalytic Hydrogen Production using meso-Tetra ferrocenyl porphyrin Palladium (II) and Copper (II) Complexes. In: **Dalton Transactions**, 2015. Accepted Manuscript.
- in journals from the National Register of profile journals:
 - **Sirbu, D.** Temperature dependence of ^{57}Fe -mössbauer spectra for a $\text{Fe}_{\text{Fc}}^{\text{II}} - \text{Fe}_{\text{tpy}}^{\text{II}} - \text{Fe}_{\text{Fc}}^{\text{II}}$ trinuclear system. In: **Chemistry Journal of Moldova. General, Industrial and Ecological Chemistry**, 2015, nr. 10 (1), p. 61-66.

Abstracts on scientific conferences:

1. **Sirbu, D.** Sinteza și caracterizarea 5,10,15,20-tetra(ferocenil) porfirinatului de paladiu(ii). In: Conferința Internațională a Tinerilor Cercetători, edition IX. Chișinău: Free International University of Moldova, 11 November 2011, p. 65;
2. Turtă, C.; **Sirbu, D.**; Benniston, A.C. Uv-vis and redox chemistry of copper 5,10,15,20-tetra(ferrocenyl) porphyrin. In: The V International Conference-Symposium "Ecological Chemistry 2012". Chișinău: Academy of Sciences of Moldova, 2-3 March 2012, p. 137-138;
3. **Sirbu, D.**; Barbă, A.; Gorincioi, E. Synthesis and NMR-characterisation of the novel 5,10-bisferrocenyl-15,20-bis(4-methoxybenzoyl) porphyrin. In: The XVII-th Conference "Physical Methods in Coordination and Supramolecular Chemistry". Chișinău: Institute of Chemistry of ASM, 24-26 October 2012, p. 188.
4. **Sirbu, D.** Synthesis and characterisation of the novel zinc(II)-5,10,15-trisferrocenyl-20-(4-carboxyphenyl) porphyrin. In: The VII National conference on chemistry and nanomaterials of young scientists, PhD and students with the international participation "Mendeleev-2013". St. Petersburg: Saint Petersburg State University, 2-5 April 2013, H-12.
5. **Sirbu, D.**; Turta, C.; Benniston, A.C. Synthesis and structure 1,1'-bis-(dipyrrromethane) ferrocene. In: Integration through research and innovation. Chișinău: Moldova State University, 26-28 September 2013, p. 94-95.
6. **Sirbu, D.** Introducing ferrocene in dye-sensitizers for solar cell applications. In: Symposium & Young-Researcher-Meeting: Current Challenges in Supramolecular Artificial Photosynthesis. Poster and oral presentation. Jena, Germany: Friedrich Schiller University, 09-13 March 2014.
7. **Sirbu, D.**; Gorincioi, E. New Polychiralic asymmetrically 1,1'-disubstituted ferrocene ligand with multiple coordination sites. In: The Intern. Conf. dedicated to the 55th anniversary from foundation of the Institute of Chemistry of the ASM. Chișinău: Institute of Chemistry of ASM, 28-30 Mai 2014, p. 137.

ADNOTARE

Sîrbu Dumitru, „Sinteza, studiul derivaților ferocenului și porfirinei și a combinațiilor coordinative ale acestora cu metalele de tranziție (Fe, Co, Ni, Cu, Zn, Ru și Pd)”. Teză de doctor în științe chimice, specialitatea 141.01 - chimia anorganică. Chișinău, 2015. Teza constă din introducere, patru capitole, concluzii generale și recomandări, bibliografie din 223 referințe și 14 anexe care conțin 24 figuri. 128 pagini text de bază conțin 90 figuri, 11 tabele și 2 ecuații. Rezultatele descrise în teză au fost publicate în 13 lucrări științifice: patru articole în reviste cu factor de impact și un articol în revistă națională de categoria B (fără coautori), un fragment al capitolului dintr-o monografie internațională, o prezentare orală și șapte abstracte (trei fără coautori) la conferințe.

Cuvinte cheie: ferocen, porfirină, complecși, metale, tranziție, celulă solară, reducerea protonilor, UV-Vis.

Scopul acestei lucrări este studiul relațiilor structură-proprietate ce ar permite înțelegerea mai profundă a mecanismelor care determină procesele fotofizice și electrochimice, în sistemele în baza porfirinei și ferocenului, pentru evidențierea potențialului aplicativ al materialelor obținute. Pentru îndeplinirea **obiectivelor** propuse au fost utilizate diferite metode contemporane, inclusiv spectroscopiile de masă, IR, RMN, absorbția atomică, analiza elementală și difracția razelor X – pentru determinarea compoziției și caracterizarea structurală a compușilor. Studiul fotofizic, electrochimic și al potențialului aplicativ a fost efectuat prin utilizarea unui șir de metode: absorbție electronică și spectroelectrochimie UV-Vis, absorbție tranzientă „pump-probe”, spectroscopie Mössbauer, voltametrie ciclică și modelare moleculară DFT.

Originalitatea științifică. Au fost obținuți 27 compuși, inclusiv 14 derivați noi ai ferocenului și porfirinei, utilizând procedeele sintetice elaborate și au fost propuse mecanismele reacțiilor. Trebuie subliniată sinteza produsului nou, derivat bis-cetopirolic al ferocenului și al complexului său cu BF₂, precum și procedeul nou pentru desimetrizarea oxidativă a moleculei de ferocen. Pentru prima dată un colorant ferocen-porfirinic a fost utilizat în calitate de sensibilizator al suprafeței de TiO₂ în celulă Grätzel și au fost analizate procesele-cheie ce determină eficacitatea sistemului. A fost propus mecanismul producerii electrochimice a hidrogenului în baza intermediarului florinic, catalizat de mezo-tetraferocenil porfirinatul de Pd(II) și Cu(II), și a fost explicat rolul unităților ferocenice.

Această lucrare oferă unele răspunsuri și concluzii cu **semnificație teoretică și o valoare aplicativă** pentru procesul de cercetare atât în echipa noastră, cât și în alte grupe ce lucrează în domenii similare sau înrudite. Metoda simplă fără cromatografie, elaborată pentru desimetrizarea moleculei de ferocen oferă o cale alternativă de obținere a derivaților 1,1'-asimetric disubstituiți ai ferocenului ce prezintă potențial de aplicare în procesele catalitice industriale. Proprietățile redox ale derivatului bis-cetopirolic al ferocenului permit aplicarea acestui material în calitate de sensibilizator redox al prezenței nucleofililor. Studiul proceselor fotoinduse în colorantul ferocen-porfirinic adsorbit pe suprafața TiO₂ prezintă o încercare de a găsi factorii limită ai DSSC, iar concluziile făcute în această lucrare vor ghida optimizarea ulterioară a celulelor solare sensibilizate cu porfirine. Complecșii mezo-tetra-ferocenil porfirinici au prezentat activitate catalitică înaltă în obținerea electrochimică a hidrogenului, oferind informație valoroasă pentru generarea materialelor alternative în reducerea electrocatalitică a protonilor.

Problema științifică soluționată constă în elucidarea relației structură-proprietate în sistemele moleculare în baza ferocenului și porfirinei, contribuind la înțelegerea mai profundă a proceselor fizice și chimice în materialele studiate, întru optimizarea ulterioară a eficienței lor aplicative.

АННОТАЦИЯ

Сырбу Думитру, "Синтез, исследование производных ферроцена и порфирина и их комплексов с переходными металлами (Fe, Co, Ni, Cu, Zn, Ru и Pd)". Диссертация доктора химических наук, специальность 141.01 - неорганическая химия. Кишинэу, 2015. Диссертация состоит из введения, четырех глав, общих выводов и рекомендаций, библиографии из 223 ссылок и 14 приложений, состоящих из 24 фигур. 128 страниц основного текста содержат 90 рисунков, 11 таблиц и два уравнения. Результаты, описанные в диссертации были опубликованы в 13 научных работах: 4 статьи в журналах с импакт-фактором, одна в журнале Б-класса (без соавторов), отрывок в главе монографии, один устный доклад и семь тезисов (три без соавторов) на научных конференциях.

Ключевые слова: ферроцен, порфирин, комплекс, солнечная ячейка, восстановление протонов, УФ-Вид.

Целью данной работы является исследование соотношений структура-свойство которые позволили бы лучше понять механизмы, регулирующие фотофизические и электрохимические процессы, в системах на основе порфирина и ферроцена, для выявления их практического потенциала. Разнообразие современных методов (ИК, ЯМР, масс спектроскопии, атомная абсорбция, элементный и рентгено-дифракционный анализ) были использованы для описания состава и структуры соединений, в то время как УФ-Вид поглощение и спектроскопия, "pump-probe" нестационарное поглощение, мессбауэровская спектроскопия, циклическая вольтамперометрия и молекулярное моделирование методом ДФТ были использованы для изучения фотофизических, электрохимических свойств и прикладного потенциала полученных материалов.

Оригинальность результатов. Были получены 14 новых производных порфирина и ферроцена и предложены механизмы реакций. Следует отметить синтез нового, трудно выделяемого кетопирольного производного ферроцена и его BF_2 хелата, а также новый простой путь для десимметризации молекулы ферроцена. Впервые ферроцен-порфириновый краситель был использован в качестве сенсibiliзирующего пигмента поверхности TiO_2 в ячейке Грәцель и были проанализированы основные процессы определяющие производительность системы. Предложен механизм электрохимического получения водорода основанный на формировании мезо-тетра-ферроценил флоринового промежуточного продукта и было предложено объяснение роли ферроцена.

Эта работа дает некоторые ответы и выводы с *теоретическим и прикладным значением*, которые, как ожидается, будут полезны для дальнейших исследований как в нашей, так и в других группах, работающих в аналогичных или смежных областях. Простой метод исключаящий хроматографию, разработанный для десимметризации молекулы ферроцена, является альтернативным маршрутом для получения 1,1'-асимметричных ферроценов, потенциально полезных в промышленных каталитических процессах. Циклическая вольтамперометрия бис-кетопирольного ферроцена показала потенциал для редокс зондирования нуклеофилов. Исследование фотоиндуцированных процессов в ферроцен-порфириновом красителе, закрепленном на поверхности TiO_2 , будет полезно для дальнейшей разработки солнечных батарей сенсibiliзированных порфиринами. мезо-Тетраферроценил порфириновые комплексы были использованы в электрохимическом получении молекулярного водорода, предоставляя ценную информацию для разработки новых альтернативных материалов для электрокаталитического восстановления протонов.

Решенная научная проблема состоит в выяснении взаимосвязи структура-свойство в молекулярных системах на основе ферроцена / порфирина, способствуя более глубокому пониманию физических и химических процессов в исследованных материалах, для дальнейшей оптимизации их практической эффективности.

ANNOTATION

Sîrbu Dumitru, „Synthesis, study of ferrocene and porphyrin derivatives and their complexes with transition metals (Fe, Co, Ni, Cu, Zn, Ru and Pd)”. PhD thesis in chemistry, speciality 141.01 - inorganic chemistry. Chişinău, 2015. Thesis consists of introduction, four chapters, overall conclusions and recommendations, bibliography of 223 references and 14 annexes comprising of 24 figures. 128 pages of main text contain 90 figures, 11 tables and two equations. The results described within this dissertation were published in 13 scientific papers: four articles in journals with impact factor and one in journal of B grade (without co-authors), part of a chapter from international book, one oral and seven poster presentations (three without co-authors) at scientific conferences.

Keywords: ferrocene, porphyrin, transition metal complexes, solar cell, protons reduction, UV-Vis.

The aim of this work is the study of structure-property relationships that would allow a better understanding of the mechanisms governing the photophysical and electrochemical processes, in the porphyrin and ferrocene based systems, in order to identify their practical potential. A variety of contemporary methods, including IR, NMR and mass spectrometries, atomic absorption, elemental and X-ray diffraction analyses, were used for molecular composition and structural characterisation of the compounds, while UV-Vis absorption and spectroelectrochemistry, pump-probe transient absorption, Mössbauer spectrometry, cyclic voltammetry and DFT molecular modeling were employed in order to study the photophysical, electrochemical and applicative properties.

The originality of results. 14 new derivatives of ferrocene and porphyrin, were obtained using elaborated synthetic protocols and the reaction mechanisms were proposed. It should be emphasized the synthesis of the new, rarely isolated ketopyrrole halfway product in the BODIPY synthesis, and its BF₂ chelate, as well as the novel simple route for oxidative desymmetrization of ferrocene molecule. For the first time a ferrocene-porphyrin dye was employed as sensitizer for TiO₂ surface in a Grätzel cell and the key processes governing the system efficiency were analysed. The mechanism for Pd(II) and Cu(II) porphyrin ring centred electrochemical hydrogen production was proposed consisting of a phlorin mediated pathway and a feasible explanation of ferrocene units role was suggested.

This work is giving some answers and conclusions with **fundamental and applicative** value, that are expected to be useful in the further research both in our and other teams working in similar or related area. The simple chromatography-free method elaborated for desymmetrizing ferrocene molecule is an alternative route to 1,1'-asymmetrical ferrocenes that could find practical applications in industrial catalytic processes. The cyclic voltammetry of bis-ketopyrrolic derivative of ferrocene proved the material to be useful for nucleophiles redox sensing. The study of photoinduced processes in ferrocene-porphyrin dye anchored on the TiO₂ surface is a trial to find the “bottleneck” of DSSCs and the conclusions made within this work will guide further design of porphyrin-sensitized solar cells. The *meso*-tetraferrocenyl porphyrin metal complexes showed catalytic activity in electrochemical generation of molecular hydrogen, giving some valuable information for generation of alternative materials for the electrocatalytic reduction of protons.

The **solved scientific problem** consists of elucidating the structure-property relationship in the molecular systems based on ferrocene/porphyrin, contributing to a deeper understanding of the physical and chemical processes in the materials studied for further optimisation of their practical efficiency.

SÎRBU DUMITRU

**SYNTHESIS, STUDY OF FERROCENE AND PORPHYRIN
DERIVATIVES AND THEIR COMPLEXES WITH TRANSITION
METALS (Fe, Co, Ni, Cu, Zn, Ru and Pd)**

141.01. INORGANIC CHEMISTRY

Summary of the doctoral thesis in chemical sciences

Approved to print: 18.06.2015
Offset paper. Offset printing.
Printing Sheets: 2.0 author sheets.

Paper size 60x84 1/16
20 copies
Order nr. 680

Centrul Editorial-Poligrafic al U.S.M.,
str. A. Mateevici 60, MD-2009, Chişinău

**INSTITUTUL DE CHIMIE
AL ACADEMIEI DE ȘTIINTE A MOLDOVEI**

Cu titlu de manuscris

CZU: 546.7:546.5:546.4(043.2)+541.13(043.2)+544.174.2(043.2)

SÎRBU DUMITRU

**SINTEZA, STUDIUL DERIVAȚILOR FEROCENULUI ȘI
PORFIRINEI ȘI A COMBINAȚIILOR COORDINATIVE ALE
ACESTORA CU METALELE DE TRANZIȚIE
(Fe, Co, Ni, Cu, Zn, Ru și Pd)**

141.01. CHIMIE ANORGANICĂ

Autoreferatul tezei de doctor în științe chimice

Chișinău 2015